

# Optical spectroscopy of X-Mega targets in the Carina nebula – VI. FO 15: a new O-type double-lined eclipsing binary

V. S. Niemela,<sup>1★†</sup> N. I. Morrell,<sup>2‡</sup> E. Fernández Lajús,<sup>1§</sup> R. Barbá,<sup>3¶</sup> J. F. Albacete Colombo<sup>4||</sup> and M. Orellana<sup>5★★</sup>

<sup>1</sup>Facultad de Ciencias Astronómicas y Geofísicas de la Universidad Nacional de La Plata, Paseo del Bosque S/N, 1900 La Plata, Argentina

<sup>2</sup>Las Campanas Observatory, Observatories of the Carnegie Institution of Washington, Casilla 601, La Serena, Chile

<sup>3</sup>Departamento de Física, Universidad de La Serena, Benavente 980, La Serena, Chile

<sup>4</sup>Osservatorio Astronomico di Palermo, Piazza del Parlamento 1, Palermo (90141), Italy

<sup>5</sup>Instituto Argentino de Radioastronomía, C.C. 5, 1894 Villa Elisa, Argentina

Accepted 2006 January 6. Received 2006 January 6; in original form 2005 November 9

## ABSTRACT

We report the discovery of a new O-type double-lined spectroscopic binary with a short orbital period of 1.4 d. We find the primary component of this binary, FO 15, to have an approximate spectral type O5.5Vz, i.e. a zero-age main-sequence (ZAMS) star. The secondary appears to be of spectral type O9.5V. We have performed a numerical model fit to the public All Sky Automated Survey photometry, which shows that FO 15 is also an eclipsing binary. We find an orbital inclination of  $\sim 80^\circ$ . From a simultaneous light curve and radial velocity solution, we find the masses and radii of the two components to be  $30 \pm 1$  and  $16 \pm 1 M_\odot$  and  $7.5 \pm 0.5$  and  $5.3 \pm 0.5 R_\odot$ . These radii, and hence also the luminosities, are smaller than those of normal O-type stars, but similar to recently born ZAMS O-type stars. The absolute magnitudes derived from our analysis locate FO 15 at the same distance as  $\eta$  Carinae. From *Chandra* and *XMM* X-ray images, we also find that there are two close X-ray sources: one coincident with FO 15 and the other one without optical counterpart. The latter seems to be a highly variable source, presumably due to a pre-main-sequence stellar neighbour of FO 15.

**Key words:** binaries: eclipsing – binaries: spectroscopic – stars: fundamental parameters – stars: individual: FO 15 – X-rays: stars.

## 1 INTRODUCTION

In their survey for OB stars in the field of the Carina nebula (NGC 3372), Forte & Orsatti (1981) discovered an early O-type star in the darkest region of the nebula. This star ( $\alpha_{2000} = 10^{\text{h}}45^{\text{m}}36^{\text{s}}$ ;  $\delta_{2000} = -59^\circ 48' 22''$ ;  $V = 12.05$ ), number 15 in their list of new OB stars, was assigned a spectral classification O4V on photographic

image tube spectrograms. The star has been named FO 15 in the subsequent literature.

In an infrared (IR) study of the stellar population in the direction of the Carina nebula, Smith (1987) identifies FO 15 as a member of a group of heavily reddened OB stars in the south-east border of the open cluster Trumpler 16, considering that these stars most probably are also members of this cluster. An anomalous reddening law characterized by a value of  $R = A_V/E(B - V) = 4.8$  is obtained by Smith (1987).

In Fig. 1, we illustrate the location of FO 15 in the Carina nebula, inside the V-shaped dust lane dividing the brightest part of the nebula, between the open clusters Trumpler 16 and Collinder 228. The  $H\alpha$  image shown in Fig. 1 was obtained in 1999 May, with the Curtis–Schmidt telescope at the Cerro Tololo Inter-American Observatory (CTIO), Chile.

FO 15 was observed as a faint X-ray source in Einstein satellite X-ray images of the Carina nebula (Chlebowski, Harnden & Sciortino 1989). Because one of the most often proposed mechanisms for producing X-rays from O-type stars is colliding stellar winds in binary systems, we decided to include FO 15 in our ongoing optical spectroscopic observations in search for O-type binaries.

\*E-mail: virpi@fcaglp.unlp.edu.ar

†Member of Carrera del Investigador, CIC-BA, Argentina; Visiting Astronomer, CASLEO, San Juan, Argentina.

‡Member of Carrera del Investigador, CONICET, Argentina, on leave from La Plata National University, Argentina; Visiting Astronomer, CASLEO, San Juan, Argentina; Visiting Astronomer, CTIO, NOAO, operated by AURA, Inc., for NSF; Visiting Astronomer, European Southern Observatory, Chile.

§Fellow of CONICET, Argentina.

¶Member of Carrera del Investigador, CONICET, Argentina, on leave from La Plata National University, Argentina.

||Post-doctoral fellow of CONICET, Argentina.

★★Fellow of CONICET, Argentina.



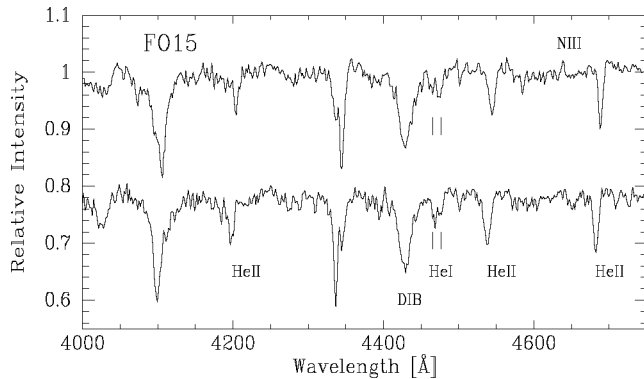


**Figure 3.** Spectra of FO 15 obtained at CASLEO in 2001 February, during orbital phases 0.78 (upper) and 0.14 (lower) showing the spectral lines of the two components seen in He I  $\lambda 4471$ . Note also the faint emission line of N III.

that the He II absorption at  $\lambda 4686$  is stronger than any of the other He II lines, a proposed signature of a zero-age main-sequence (ZAMS) luminosity class (Vz) for O-type stars (cf. Walborn & Blades 1997 and references therein).

A visual inspection of our first spectra of FO 15 which we obtained at CASLEO in 1996 December, during successive nights, showed that the stellar hydrogen absorption lines moved from the blue side to the red side of the nebular emissions, a signature of a rather high-amplitude orbital motion in a binary system. This was confirmed with further observations, which also showed that the neutral helium lines appeared double at maximum velocities, but ionized helium lines always appeared single, as shown in Fig. 3, which depicts two spectra obtained at CASLEO during approximately opposite orbital phases of the binary (see below).

The spectrum of FO 15 appears somewhat variable, as occasionally faint N III emission at  $\lambda 4634-40$  appears, as seen in the upper spectrum of Fig. 3. However, the radial velocities of this emission do not clearly correspond to any of the binary components, and it may arise in the zone of interaction of the close components.

Nebular emission lines are observed in our spectra along with nebular He I  $\lambda 3888$  absorption. The interstellar absorption lines of Ca II and Na I appear multiple. These are common features observed towards the giant H II region of Carina (e.g. Walborn & Hesser 1975; Walborn et al. 2002). The main components of Ca II absorption in our Echelle spectra have a heliocentric radial velocity of  $+7 \pm 1 \text{ km s}^{-1}$ , the nebular [O III]  $\lambda 5007$  emission a velocity of  $-19 \pm 2 \text{ km s}^{-1}$  and the nebular He I  $\lambda 3888$  absorption of  $-22 \pm 2 \text{ km s}^{-1}$ . We have used these velocities to check the consistency of the stellar radial velocities derived from our lower resolution spectra.

### 3.1 Spectral types of the binary components

Spectral classification of components in a close binary systems is not as straightforward task as classifying spectra of single stars. In very close systems of hot stars, such as FO 15, mutual heating effects may introduce a spectral appearance with hotter effective temperature. Furthermore, spectral variations due to the interaction of stellar winds of the components are often observed.

We have chosen the usual approach to classify the binary components of FO 15 in the spectrograms observed when the spectral lines have their maximum separation. To determine the spectral types, we measured in our higher resolution spectra the equivalent widths of the He I and He II lines. We then used the quantitative classification

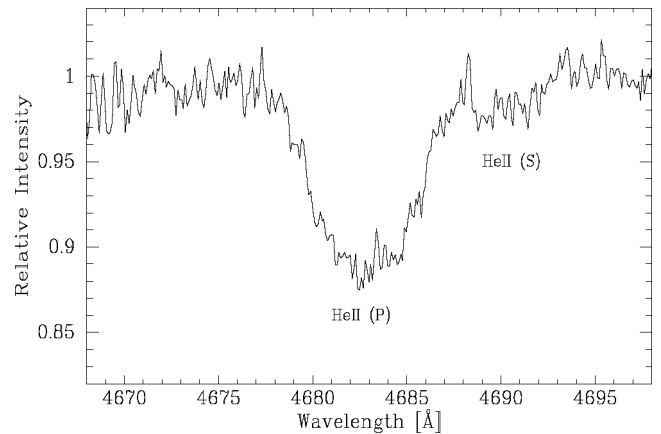


**Figure 4.** Continuum-normalized spectrum of FO 15, obtained with MIKE at the Magellan II telescope in 2002 December (orbital phase 0.34), showing the He II  $\lambda 4686$  absorption lines of both binary components.

criteria for O-type stars as described by Conti & Alschuler (1971), comparing the equivalent widths of He I  $\lambda 4471$  with He II  $\lambda 4542$ . We also compared He I  $\lambda 4922$  with He II  $\lambda 5411$ , as suggested by Kerton, Ballantyne & Martin (1999). According to these criteria, we obtained for the primary component of FO 15 a spectral classifications of O5.5V.

We note, however, that the spectrum observed near the orbital phase when the primary star is in front of the system (see Fig. 2), and the contribution of the secondary to the spectrum is expected to be minor, corresponds to a spectral type about one subtype later than O5.5, when compared with the digital spectral atlas of O-type stars published by Walborn & Fitzpatrick (1990).

The spectral type of the secondary component is more difficult to ascertain. He II absorptions corresponding to the secondary component is not observed in our lower resolution spectra, as is evident in Fig. 3. In our high-resolution spectra, all the He I absorptions appear as double lines, but only the He II  $\lambda 4686$  line corresponding to the secondary component is clearly observed. Both components of this line are shown in Fig. 4. He II  $\lambda 5411$  absorption of the secondary component may also be present, but it appears blended with the diffuse interstellar bands at  $\lambda \lambda 5404$  and  $5420$ . The spectral type of the secondary component is probably O9.5V, but could be slightly later.

We do not observe in our optical spectra of FO 15 any mass-loss indicators (signs of strong stellar winds), such as those listed, e.g. by Hutchings (1978). The Balmer H $\alpha$  line is observed in absorption in both binary components, as illustrated in Fig. 5. The radial velocity of this absorption agrees with the values derived from He lines, indicating that the H $\alpha$  absorption is mostly photospheric, and not formed in the accelerated part of an expanding atmosphere. Thus, FO 15 may be composed of weak-wind and low mass-loss rate O-type dwarfs, as those recently discussed by Martins et al. (2005b).

## 4 THE RADIAL VELOCITY ORBIT

To determine the radial velocity orbit of the binary, we measured the radial velocities of the He lines in the spectra of FO 15 fitting Gaussian profiles to the spectral lines within the IRAF routine SPLIT. The results are listed in Table 1. The radial velocities of the primary component are mostly based on the velocities of He II absorptions, and the velocities of the secondary on those of He I. To calculate

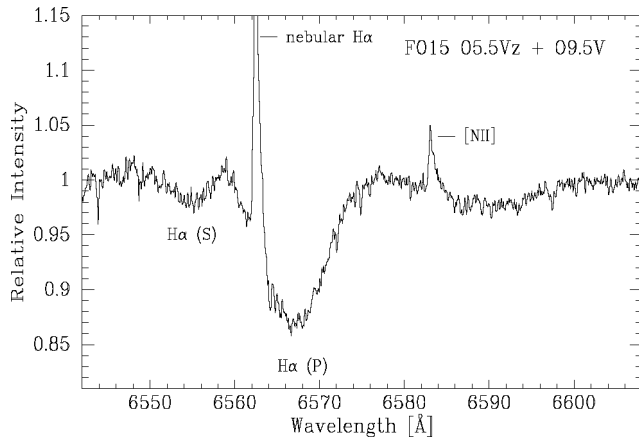


**Figure 5.** Continuum-normalized spectrum of FO 15, obtained with MIKE at the Magellan I telescope in 2003 May (orbital phase 0.81), showing the H $\alpha$   $\lambda$ 6563 absorption lines of both binary components. Nebular emissions of H $\alpha$  and [N II] are also indicated in the spectrum.

**Table 1.** Observed heliocentric radial velocities for the primary and secondary components of FO 15. Radial velocities (RV) and (O–C) values are in km s $^{-1}$ .

HJD (days)	Phase	Primary		Secondary	
240 0000+	$\phi$	RV	O–C	RV	O–C
50125.751 <sup>a</sup>	0.57	102	–7		
50127.747 <sup>a</sup>	0.98	–4	14		
50128.758 <sup>a</sup>	0.70	222	10	–423	25
50129.694 <sup>a</sup>	0.36	–165	9		
50471.804 <sup>a</sup>	0.38	–180	–28		
50472.773 <sup>a</sup>	0.07	–148	–15		
50473.778 <sup>a</sup>	0.78	204	–3	–431	8
50477.807 <sup>a</sup>	0.63	167	–1		
50478.774 <sup>a</sup>	0.31	–233	–15		
50854.825 <sup>a</sup>	0.34	–211	–18		
50858.785 <sup>a</sup>	0.14	–218	–6	367	6
50860.749 <sup>a</sup>	0.53	15	–45		
50861.739 <sup>a</sup>	0.23	–247	–1	426	–1
51355.466 <sup>a</sup>	0.51	18	–11		
51653.594 <sup>a</sup>	0.42	–93	13		
51654.551 <sup>a</sup>	0.10	–173	–7		
51718.487 <sup>a</sup>	0.33	–206	2	361	8
51959.799 <sup>a</sup>	0.04	–109	–15		
51960.842 <sup>a</sup>	0.78	199	–9	–452	–11
51961.765 <sup>a</sup>	0.43	–76	16		
51962.776 <sup>a</sup>	0.14	–219	–8	369	9
52251.847 <sup>b</sup>	0.64	179	–1	–382	5
52298.849 <sup>a</sup>	0.89	106	–3		
52302.856 <sup>a</sup>	0.73	202	–14	–439	18
52329.604 <sup>a</sup>	0.65	196	10	–386	12
52332.820 <sup>a</sup>	0.93	80	12		
52628.844 <sup>c</sup>	0.34	–192	2	345	18
52690.606 <sup>a</sup>	0.04	–113	–24		
52766.626 <sup>c</sup>	0.81	200	12	–399	2
52836.495 <sup>d</sup>	0.24	–225	25	420	–6

Notes. Data origin: <sup>a</sup>CASLEO, <sup>b</sup>ESO-VLT, <sup>c</sup>LCO Magellan, <sup>d</sup>LCO du Pont phases have been calculated according to the ephemeris HJD ( $\phi = 0$ ) = 245 2837.565 + 1.413 56E.

the orbital parameters, we used a modified version of the program originally written by Bertiau & Grobber (1969), introducing the period determined by ASAS photometry, namely 1.4136 d as an initial value. We assigned higher weight to the higher resolution

**Table 2.** Parameters of circular radial velocity orbit for FO 15.

	Primary	Secondary
$P$ (days)	1.413 56 $\pm$ 0.000 003	
$V_o$ (km s $^{-1}$ )	–15 $\pm$ 2	
$a \sin i$ (R $_{\odot}$ )	6.42 $\pm$ 0.05	12 $\pm$ 0.05
$K$ (km s $^{-1}$ )	231 $\pm$ 2	442 $\pm$ 3
$M \sin^3 i$ (M $_{\odot}$ )	29 $\pm$ 1	15 $\pm$ 1
$T_o$ (HJD) 245 0000+	3159.5 $\pm$ 0.2	3150.7 $\pm$ 0.2

observations and to those obtained near quadratures. The orbital parameters are listed in Table 2, along with their formal standard errors as calculated by the above-mentioned program.

Our radial velocities define a circular orbit within the errors, the calculated orbital eccentricity being  $e = 0.05 \pm 0.06$ . This is as expected for a massive binary with such a short orbital period, as is the case for FO 15.

## 5 LIGHT CURVE ANALYSIS

Photometric V filter data of FO 15 were reported by the ASAS in Pobjmański (2003). This star is catalogued as ASAS 104536-5948.4 in the ASAS catalogue of variable stars, being classified as an eclipsing binary with a period of  $P = 1.^d4136$ . A visual inspection of the ASAS light curve of FO 15 shows periodic light variations with a rather large apparent scatter of data, almost  $\pm 0.1$  mag over all orbital phases. In order to obtain a first estimation of the orbital inclination  $i$  of the binary system, we have attempted to fit a numerical eclipsing binary model to the ASAS observations, using the Wilson–Devinney (W–D) code (Wilson & Devinney 1971; Wilson 1990; Wilson & Van Hamme 2004). ASAS photometric data and our radial velocities were used to compare with the results of the model fitting.

We set the W–D code in mode 2 for detached binaries with no constraints on the potentials (except the luminosity of the secondary). The simplest considerations were applied for the emission parameters of the stars in the model, i.e. the stars as black bodies and the approximate model reflection (MREF = 1). No third light or spots were included. We adopted gravity darkening exponents  $g_1 = g_2 = 1$ , and bolometric albedos  $Alb_1 = Alb_2 = 1$  were set for radiative envelopes. We used the square root limb darkening law. Limb darkening coefficients for visual wavelengths were taken from Díaz-Cordovés, Claret & Giménez (1995) and bolometric limb darkening coefficients from Van Hamme (1993). We adopted the period  $P = 1.^d41356$  and mass ratio  $M_2/M_1 = 0.52$  from the radial velocity orbit (cf. Table 2). For both binary components, effective temperatures corresponding to their spectral types were adopted from the compilation by Martins, Schaerer & Hillier (2005a), i.e.  $T_{\text{eff}1} \sim 40\,000$  K and  $T_{\text{eff}2} \sim 32\,000$  K for the primary and secondary components, respectively. We assumed that the system has a circular orbit ( $e = 0$ ) with both components rotating synchronously ( $F_1 = F_2 = 1$ ), as suggested by the observations and as expected for a massive binary with a short period, as is the case for FO 15. With all of these parameters fixed, we generated synthetic light and radial velocity curves adjusting them to the observations. We used the PHOEBE package (Prša & Zwitter 2005) which incorporates numerical innovations and technical aspects to the W–D code. The results for the best fit, optimized by the code, are shown in Figs 6 and 7 and listed in Table 3.

With the inclination of the orbital plane, which we found to be  $i = 80^\circ \pm 1^\circ$ , the values of the stellar masses for the components

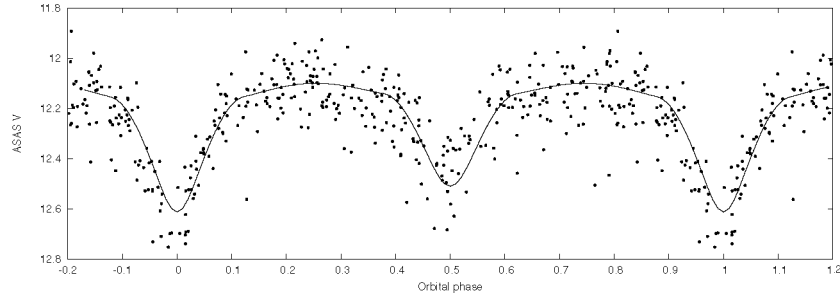


**Figure 6.** ASAS V light curve of FO 15. The continuous line represents our best-fitting W–D model.

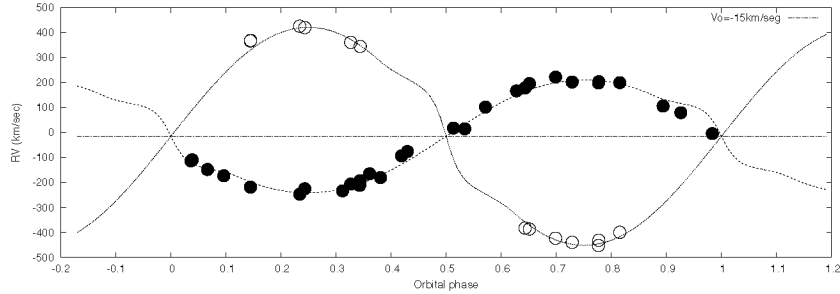


**Figure 7.** Observed radial velocities of the primary (filled circles) and secondary (open circles) of FO 15 as a function of the orbital phase. The continuous curves represent the radial velocity orbit obtained from the W–D model fitting.

**Table 3.** Astrophysical data for the binary components of FO 15 derived from the best-fitting W–D model.  $R_L$  stand for the effective radius of the Roche lobe.

Parameters	Component	
	Primary	Secondary
$P$ (days)	$1.413\,56 \pm 10^{-5}$	
$i$ ( $^\circ$ )	$80 \pm 1$	
$a$ ( $R_\odot$ )	$19 \pm 0.3$	
$M$ ( $M_\odot$ )	$30.4 \pm 1$	$15.8 \pm 1$
$M_2/M_1$	0.52*	
$R_{\text{mean}}$ ( $R_\odot$ )	$7.5 \pm 0.5$	$5.3 \pm 0.5$
$R_L$ ( $R_\odot$ )	8.3	6.15
$T_{\text{eff}}$ (K)*	40000	32000
$M_{\text{bol}}$	$-7.98 \pm 0.02$	$-6.27 \pm 0.02$
$L_2/L_1$	$0.35 \pm 0.01$	
$\text{Log } g$ (cgs)	$4.17 \pm 0.01$	$4.19 \pm 0.05$

\* Fixed.

of FO 15  $M_1 = 30.4 \pm 1 M_\odot$  and  $M_2 = 15.8 \pm 1 M_\odot$ , are in fair agreement with the tabulations by Martins et al. (2005a) based on models of stellar atmospheres.

However, the stellar mean radii that we have obtained, namely  $R_1 = 7.5 \pm 0.5 R_\odot$  and  $R_2 = 5.3 \pm 0.5 R_\odot$  for the primary and secondary components, respectively, are about 30 per cent smaller than the tabulated values, hence the bolometric luminosities implied from our light curve solution are also lower.<sup>2</sup> This is similar to what was observed for another O-type binary system in the Carina nebula, namely Tr16-104 by Rauw et al. (2001), who interpreted

<sup>2</sup> A lower  $T_{\text{eff}}$  for the secondary component, would it be, e.g. of spectral type B0V, does not modify this result beyond the quoted error bars.

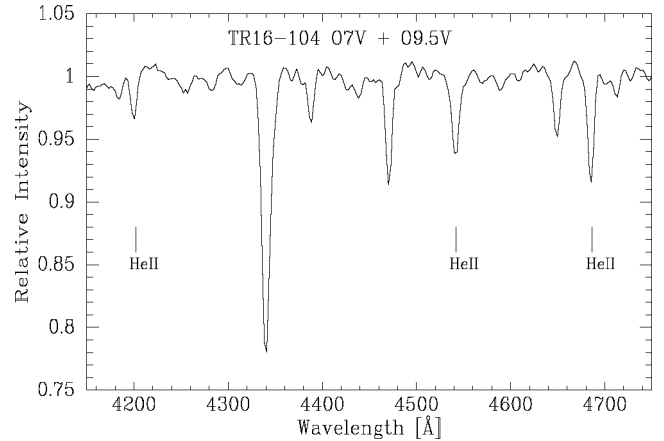


**Figure 8.** Continuum-normalized spectrum of Tr16-104 obtained at CASLEO in 1998 February, showing the signature of Vz characteristic. Absorption lines of He II  $\lambda\lambda$ 4200, 4541 and 4686 are identified.

the observations as due to fainter absolute magnitudes for stars just entering to the main sequence, i.e. stars of luminosity class Vz. In fact, the spectrum of Tr16-104 also exhibits the spectral signature of ZAMS O-type stars, namely that He II  $\lambda$ 4686 absorption is stronger than other He II lines, as is illustrated in Fig. 8.

The case may apply also to FO 15 but for a more reliable assessment of this problem, an improved and less noisy light curve is needed, and is currently being obtained (Fernández Lajús et al., in preparation).

## 6 FO 15 IN THE CARINA NEBULA

Based on their proximity in the sky, Forte & Orsatti (1981) assumed that FO 15 belongs to the open cluster Tr16, of which  $\eta$  Car is the

brightest member. However, the line of sight in this direction of the Galaxy goes almost parallel to the Sagittarius–Carina spiral arm, which is rich in young stellar population. An O5V-type star with the colours and apparent magnitude as those observed for FO 15 would have a spectrophotometric distance of  $\sim 5$  kpc if normal interstellar extinction is assumed. This would place FO 15 well behind the Carina nebula and clusters embedded within. On the other hand, it is well known that the total-to-selective extinction ratio ( $R$ ) in the direction of Carina nebula is anomalous (e.g. Smith 1987; Tapia et al. 1988). Therefore, we decided to determine the value of  $R$  for FO 15 using the published  $UBV$  photometry from Forte & Orsatti (1981) and IR magnitudes from the 2MASS (2-Micron All-Sky Survey) All-Sky Catalogue of point sources (Cutri et al. 2003).

We used the code CHORIZOS developed by Maíz Apellániz (2004) to derive the value of  $R$  for FO 15. CHORIZOS is a code that uses  $\chi^2$  minimization to find all models of energy distribution compatible with an observed data set in the  $N$ -dimensional model parameter space, which in our case are broad-band photometry and spectral type. For a complete description of the method, see Maíz Apellániz (2004). We considered TLUSTY (Lanz & Hubeny 2002) atmosphere models for the spectral energy distribution (SED) of O-type stars. An effective temperature of  $T_{\text{eff}} = 40\,000$  and  $\log g = 4.0$  were adopted to constrain the models. Using the six-colour photometry ( $UBVIJK$ ), we derived a colour excess  $E(4405\text{--}5495) = 1.21 \pm 0.02$  and a ratio of total-to-selective extinction  $R_{5495} = 4.15 \pm 0.09$ , which are the monochromatic equivalents to the usual  $E(B - V)$  and  $R_V$ , respectively. The main source of error comes from the adopted values of the magnitudes, which were obtained at different epochs, and therefore they could correspond to different orbital phases and be affected by the photometric variations of the binary system.

With the bolometric magnitudes derived from our light curve analysis, and assuming that the bolometric corrections corresponding for the spectral types as listed by Martins et al. (2005a), hold for the FO 15 binary components, we obtain absolute visual magnitudes of  $-4.2$  and  $-3.2$  for the primary and secondary, respectively. These values are about 1-mag fainter than those tabulated by Martins et al. (2005a) for stars of spectral types O5.5V and O9.5V, but are in closer agreement with the absolute magnitudes for ZAMS O-type stars as tabulated by Hanson, Howarth & Conti (1997). The values of absolute magnitudes of the binary components that we have obtained coupled with the total-to-selective extinction ratio  $R = 4.15$  derived above, would locate FO 15 at a distance of 2.2 kpc. This is coincident with the distance derived for  $\eta$  Car by Davidson

et al. (2001) based on spatially resolved Doppler velocities of the bipolar ejecta.

FO 15 is located in the region of the Carina nebula named south pillars by Smith et al. (2000) (see fig. 1) recently imaged by the Spitzer Space Telescope. Newborn stars in dust pillars pointing to  $\eta$  Car are observed in the IR image of Spitzer (Smith et al. 2005). If FO 15 is at the same distance, it can be considered as a ZAMS star embedded in an active star formation region.

## 7 X-RAY DATA

As mentioned previously, FO 15 was detected as an X-ray source in EINSTEIN observations of the Carina nebula. Subsequent X-ray data of FO 15 were observed by the ROSAT satellite in the context of the X-Mega international campaign (cf. Corcoran 1996) which also involves spectroscopic observations of hot stars with detectable X-ray emission. The ROSAT–HRI (High Resolution Imager) image shows a weak X-ray emission at the position of FO 15, considerably weaker than expected on the basis of the first EINSTEIN observation of this star, thus suggesting a variable X-ray source.

In further X-ray observations by the XMM–Newton satellite, FO 15 appeared as a hard X-ray source (Albacete-Colombo, Méndez & Morrell 2003). However, in their analysis of an X-ray image of  $\eta$  Carinae region obtained by the Chandra satellite, Evans et al. (2003) did not mention FO 15 in their list of sources with OB optical counterparts. In their list of detected sources without optical counterparts, the source number 106 appears close to FO 15 but with a difference of over 10 arcsec in the published positional coordinates. Although FO 15 is observed near the borders of the X-ray images, which all had  $\eta$  Carinae as the aimpoint, a positional difference larger than 10 arcsec seemed improbable. Therefore, we decided to re-examine the Chandra X-ray image in order to see if there might be some instrumental problem in the non-detection of FO 15 in this image. The result is depicted in Fig. 9, which shows two very close X-ray sources, the southern one is coincident with FO 15 and the northern one with source 106 of Evans et al. (2003). This source does not appear in the X-ray image of XMM satellite used by Albacete-Colombo et al. (2003), as seen in Fig. 9. Therefore, it is most probably a variable source due to a pre-main-sequence star located in the vicinity of FO 15. Indeed, Evans et al. (2003) already have suggested that the X-ray sources without optical counterparts, such as their source 106 close to FO 15, are probably pre-main-sequence stars.

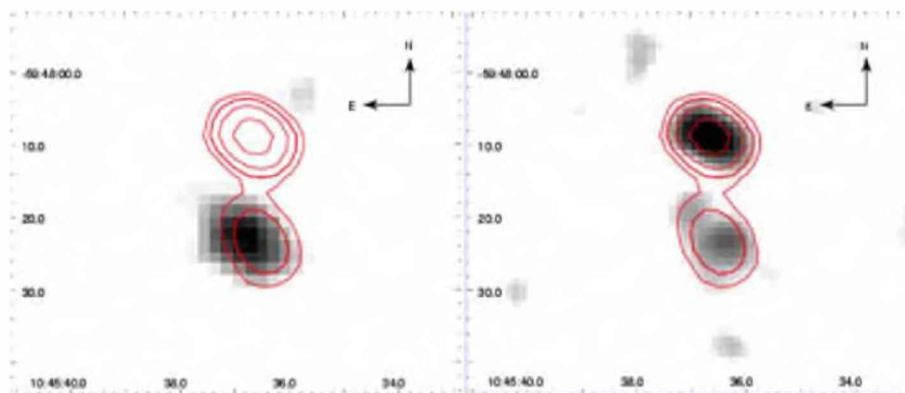


**Figure 9.** Portions of X-ray images of the Carina nebula field surrounding FO 15 observed by XMM (left-hand panel) and Chandra (right-hand panel) satellites. Contours corresponding to 0.05, 0.8, 1.5 and 3 of the background counts of the Chandra image are superposed to the grey-scale images. The brighter source to the N of FO 15 in the Chandra image is the source 106 in Evans et al. (2003). This source is absent in the image obtained by XMM.

As mentioned above, X-ray flux variability seems to be present in this system. Albacete-Colombo & Micela (2005) have studied the X-ray emission of FO 15 in the 0.4–10 keV energy range, revealing the existence of long-term X-ray variability. Higher and lower unabsorbed X-ray flux limits are between  $15.8 \times 10^{-13}$  and  $0.96 \times 10^{-13}$  erg s<sup>-1</sup>, implying  $L_x/L_{\text{bol}}$  ranges from  $9.0 \times 10^{-7}$  to  $0.54 \times 10^{-7}$ , respectively. These authors also discuss the origin of the observed hard X-ray photons as inverse Compton scattering, and confirm the existence of soft (0.2–1.2 keV) short-term variability (~25 per cent of the total flux).

## 8 SUMMARY OF THE RESULTS

(i) We have discovered that the O-type star FO 15 immersed in the active star formation site called ‘southern pillars’ in the Carina nebula is a short-period eclipsing binary.

(ii) Both binary components are visible in the spectrum, the secondary component showing considerably weaker lines.

(iii) We classify the primary spectrum as O5.5Vz, i.e. as an early-type ZAMS star. The secondary seems to be of spectral type O9.5V.

(iv) Analysis of the ASAS light curve of FO 15 fitting a binary model by the W–D method yields an orbital inclination of  $\sim 80^\circ$ .

(v) The stellar masses of the components are  $\sim 30$  and  $16 M_\odot$ .

(vi) Simultaneous light and radial velocity curve analysis yields components with smaller radii and fainter absolute magnitudes when compared with normal galactic O-type stars. These values are in agreement with recently born ZAMS O-type stars.

(vii) An individual determination of total-to-selective extinction ratio ( $R$ ) for FO 15 yields a value of 4.15, which coupled with the values of absolute magnitudes determined from the light curve locates FO 15 at a distance of 2.2 kpc, coincident with that of  $\eta$  Car.

(viii) A *Chandra* X-ray image shows two close sources at the position of FO 15. Presumably, the northern source is a pre-main-sequence star with an occasional high X-ray state, as this source apparently is not visible in the X-ray image of the same location observed by the *XMM* satellite.

## ACKNOWLEDGMENTS

We are indebted to Roberto Gamen for kindly obtaining four spectra of FO 15 for this study. We thank the directors and staff of CASLEO, LCO, CTIO and ESO, for the use of their facilities. We also acknowledge the use at CASLEO of the CCD and data acquisition system partly financed by US NSF grant AST-90-15827 to R. M. Rich. This research has received financial support from IALP, CONICET, Argentina. VSN and EFL thank CIC-BA for travel support. RB has received financial support from FONDECYT No 1050052. MO is

grateful for financial support from UNLP in the form of a research studentship. We thank the referee, Dr C. Evans, for useful comments which have improved the presentation of this paper.

## REFERENCES

- Albacete-Colombo J. F., Méndez M., Morrell N. I., 2003, *MNRAS*, 346, 704  
 Albacete-Colombo J. F., Micela G., 2005, in Rauw G., Naze Y., Blomme R., Gosset E., eds, Proc. Joint European and National Astronomical Meeting (JENAM), Massive Stars and High-Energy Emission in OB Associations, p. 69  
 Bernstein R., Shtetman S. A., Gunnels S. M., Mochnacki S., Athey A. E., 2003, *SPIE*, 4841, 1694  
 Bertiau F., Grobben J., 1969, *Ric. Spec. Vaticana*, 8, 1  
 Chlebowski T., Hamden F. R., Sciortino S., 1989, *ApJ*, 341, 427  
 Conti P. S., Alschuler W. R., 1971, *ApJ*, 170, 325  
 Corcoran M. F., 1996, *Rev. Mex. Astron. Astrofis. Ser. Conf.*, 5, 54  
 Cutri R. et al., 2003, *The 2MASS All-Sky Catalog of Point Sources*. Univ. Massachusetts and IPAC, Pasadena  
 Davidson K., Smith N., Gull T. R., Ishibashi K., Hillier D. J., 2001, *AJ*, 121, 1561  
 Díaz-Cordovés J., Claret A., Giménez A., 1995, *A&A*, 110, 329  
 Evans N., Seward F., Krauss M., Isobe T., Nichols J., Schlegel E., Wolk S., 2003, *ApJ*, 589, 509  
 Forte J. C., Orsatti A. M., 1981, *AJ*, 86, 209  
 Hanson M. M., Howarth I. D., Conti P. S., 1997, *ApJ*, 489, 698  
 Hutchings J. B., 1978, *Int. Astron. Union Symp.*, 83, 3  
 Kerton C. R., Ballantyne D. R., Martin P. G., 1999, *AJ*, 117, 2485  
 Lanz T., Hubeny I., 2002, *ApJS*, 146, 417  
 Maíz Apellániz J., 2004, *PASP*, 116, 859  
 Martins F., Schaerer D., Hillier D. J., 2005a, *A&A*, 436, 1049  
 Martins F., Schaerer D., Hillier D. J., Meynadier F., Heydari-Malayeri M., Walborn N. R., 2005b, *A&A*, 441, 735  
 Pojmański G., 2003, *Acta Astron.*, 53, 341  
 Pršša A., Zwitter T., 2005, *ApJ*, 628, 426  
 Rauw G., Sana H., Antokhin I., Morrell N., Niemela V., Albacete Colombo J. F., Gosset E., Vreux J.-M., 2001, *MNRAS*, 326, 1149  
 Smith R. G., 1987, *MNRAS*, 227, 943  
 Smith N., Egan M. P., Carey S., Price S. D., Morse J. A., Price P. A., 2000, *ApJ*, 532, L145  
 Smith N. et al., 2005, in *NASA Spitzer Space Telescope Press release 2005*, May 30  
 Tapia M., Roth M., Marraco H., Ruiz M. T., 1988, *MNRAS*, 232, 661  
 Van Hamme W., 1993, *AJ*, 106, 2096  
 Walborn N. R., Hesser J. E., 1975, *ApJ*, 199, 535  
 Walborn N. R., Fitzpatrick E. L., 1990, *PASP*, 102, 379  
 Walborn N. R., Blades J. C., 1997, *ApJS*, 112, 457  
 Walborn N. R., Danks A. C., Vieira G., Landsman W. B., 2002, *ApJS*, 140, 407  
 Wilson R. E., 1990, *ApJ*, 356, 613  
 Wilson R. E., Devinney E. J., 1971, *ApJ*, 166, 605  
 Wilson R. E., Van Hamme E. J., 2004, *Computing Binary Star Observables*. Available at <ftp://ftp.astro.ufl.edu/pub/wilson/lcdc2003/>

This paper has been typeset from a  $\text{\TeX}/\text{\LaTeX}$  file prepared by the author.